Kinetic simulations of W impurity transport by ELMs

D.C. van Vugt[1,3], _G.T.A. Huijsmans[1,2]_ _M. Hoelzl[4]_, _L.P.J. Kamp[1]_,
N.J. Lopes Cardozo[1], _A. Loarte[3]_, _ASDEX Upgrade Team[4]_
[1]Eindhoven University of Technology, Eindhoven, The Netherlands
[2]CEA Cadarache, IRFM, 13108 St. Paul Lez Durance, France
[3]ITER Organization, 13067 St. Paul Lez Durance, France
[4]Max Planck Institute for Plasma Physics, Boltzmannstr. 2, 85748 Garching b. M., Germany

Introduction

Tokamak operation with a tungsten (W) wall has many advantages in the form of better lifetimes and lower fuel retention. The main drawbacks are a possibility of melting the wall and the low allowable concentration of W ions in the plasma. Accumulation in the core plasma leads to fuel dilution and increased radiative losses that can lead to the loss of the H-mode and to thermal collapse of the plasma and a disruption in tokamaks. Concentrations in the range of a few 10^{-5} are expected to significantly decrease fusion performance in ITER and next step devices [1].

This pollution must be controlled to have H-mode operation, for instance by triggering frequent ELMs by vertical kicks or pellet injection. ELMs at sufficiently high frequency are required to prevent W accumulation in the core [2], by expelling impurities from the edge plasma region [3]. This is more effective for high-Z impurities given the large inwards pinch that they are subject to and the ensuing edge impurity density peaking. The effect of ELMs on high-Z impurity outflux in ITER remains uncertain given the expected impurity screening in the plasma pedestal [4].

Asides from preventing accumulation in the core ELMs also play a role in creating impurities. The higher heat fluxes and temperatures in the divertor region during an ELM greatly increase the sputtering yields and cause most of the impurity production. This presents a limit to the allowable power fluxes onto the divertor. Recent work [4] indicates that for the expected hollow tungsten profiles in the edge transport barrier in ITER the requirements for impurity production are less strict than those for divertor lifetime control.

For hollow impurity density profiles the effect of ELMs is not to decrease the core impurity density but rather to increase it. To investigate the physics mechanisms of the impurity transport due to ELMs we will use a kinetic model for impurity transport in the electromagnetic fields in a tokamak during an ELM. First we introduce the models used to simulate W impurity transport, and the coupling with the JOREK code. Then we investigate the transport of locally thermal W due to an (simulated) ELM in a JET-like and an ASDEX Upgrade (AUG [5]) plasma. The transport mechanisms are identified and specific regions of displaced particles are found.

Simulating W test particle transport with JOREK

In this work we use an extension of the MHD code JOREK [6] that allows the simulation of impurity transport during ELMs and thus can provide an evaluation of their effectiveness for impurity expulsion. It includes full-orbit tracking of impurities in time-varying electromagnetic fields. Ionization, recombination and radiation processes for impurities are taken into account, using the atomic data from the ADAS database. All charge states of the impurities are retained. The particles do not have a back reaction to the plasma.

This extended model has been applied to ELM simulations of a JET-like plasma and to a realistic AUG plasma [7], where we have quantified the displacement of W particles across

flux surfaces during an ELM. Figure 1 shows the projection of some characteristic particle paths onto the poloidal plane during 1ms of a JET-like ELM. Chaotic paths are observed, with particles making large radial excursions. The change in orbits is largely due to the electric field perturbations induced by the ELM (i.e. related to the ExB velocity of the formation and ejection of filaments due to unstable peeling-ballooning modes). The effect of the ergodicity of the magnetic field on the impurity transport is less important due to the low parallel velocities (due to the high impurity mass). Note that most W atoms due not complete one full banana orbit during the timescale of an ELM.
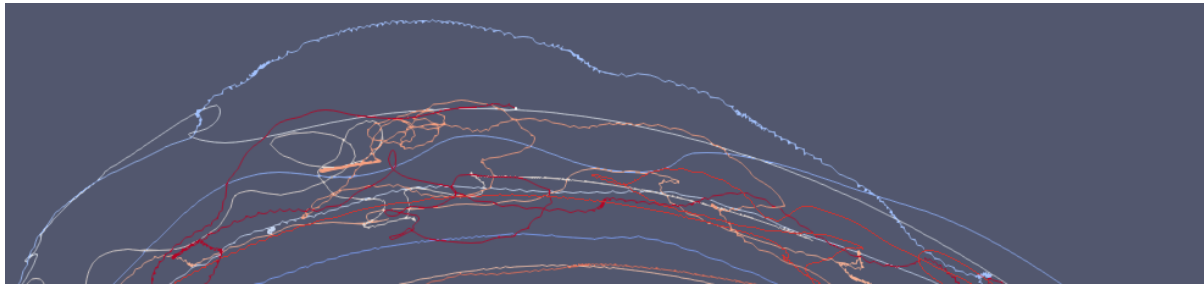
Figure 1 Particle paths projected onto a poloidal cross-section, showing only the top of the plasma.

Displacement in $\bar{\psi}$ of a uniform particle distribution in an AUG ELM [6]

The pre-ELM initialization of the W distribution needs to be as close to a steady state as possible to avoid transport not related to ELM activity. The particle positions are initialized using rejection sampling to obtain a predefined density profile. The velocities are distributed as a local Maxwellian, shifted to account for a parallel velocity. A quasi-random low discrepancy Sobol sequence is used to reduce the noise. The initial charge state is taken from the coronal equilibrium at the local temperature.

The (change in) radial position of the impurities is analysed in terms of the variable $\bar{\psi} = P_\varphi / q$, defined as the generalized toroidal momentum P_φ divided by the charge state q.

In figure 2 we show the displacement of particles starting at a specific position $\bar{\psi}$ over time during an ELM simulation in AUG discharge #33616 (q_{95}=5.8, I_{tor}=800kA, n_{e0}=7.5x10^{19}m^{-3}). The n=6 toroidal harmonic is the most unstable mode in the initial linear phase. During the ELM, the n=2-5 are dominant. The simulated ELM has an energy loss of 2.5% and a density loss of 7 %. It is clearly visible that particles in the edge region are displaced over large distances, of up to 8% of the plasma radius. Particles outside the separatrix are drawn inwards and vice versa. The ELM perturbation can be seen to act first mostly outside the pedestal and after 0.3ms also more inwards, roughly up to the line marked 'elm penetration depth'. This penetration depth is consistent with the width of the magnetic perturbation of the ELM MHD instability [6].

The effect on the particle distribution is seen to be caused by the electric fields during the ELM. Performing the same simulations but artificially disabling the electric field, leads to an average displacement on the order of 0.4% of the plasma radius.

To investigate in more detail the time-dependence of the particle displacement we look at the rate of change of the average particle displacement and of the mean-square particle displacement in figure 3. Here the radial localisation of the mode is clearly visible, as well as the strong time-dependence matching the peaks in mode energies, corresponding to moments of strongest electric field. The time evolution of the toroidal mode energies during this ELM simulation are shown in figure 4.
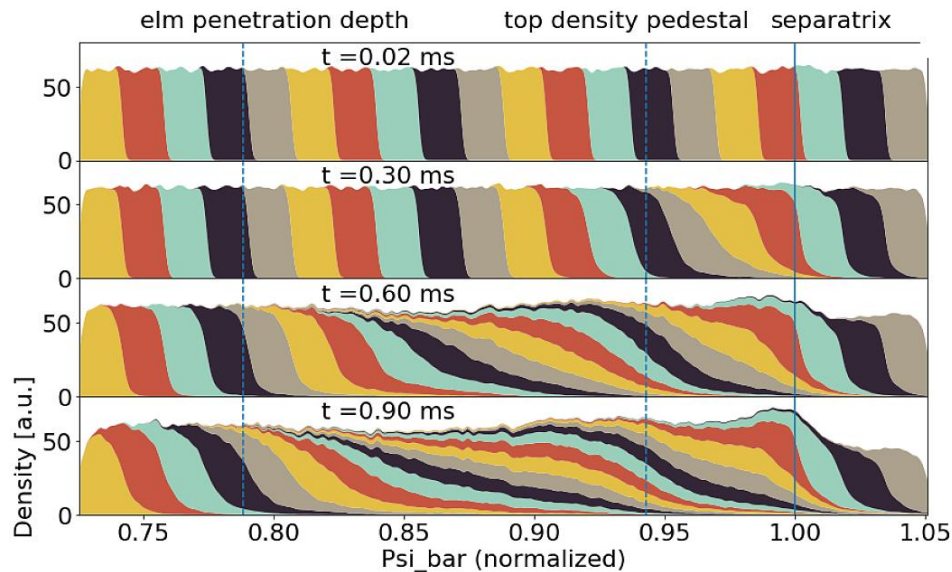
Figure 2: Particles colored for initial coordinate in $\bar{\psi}$ over time during an AUG-like ELM.

Toroidal-angle dependence of radial particle motion

Since the ballooning-mode perturbation is aligned with magnetic field lines particles that are on the same field line will experience similar fields. This leads us to believe that the field line, which can be characterized by its flux coordinate and the toroidal angle of where is crosses the outer midplane, φ_0, is a useful coordinate to investigate particle radial motion. To find this effect we trace the fieldline starting from each particle's guiding center to the outer midplane to find φ_0. Figure 5 shows the average radial velocity of particles with a specific φ_0 during the ELM over time. In the first 400 microseconds the linearly most unstable n=6 mode is clearly visible. After that the particles chaotic fields move the particles enough to remove any correlation with initial angle φ_0.

Conclusions and future work

The simulation of W test-particles during an ELM shows that their displacement is due to ExB flows from the peeling-ballooning MHD instabilities in the pedestal. Particles move with an maximum RMS displacement of 0.05 in normalized $\bar{\psi}$ in the edge, between 0.8 and 1 in $\bar{\psi}$. The impurities follow the interchange type motion of the MHD instability: a fraction of the particles localized inside the separatrix are ejected and particles outside the separatrix can move into the plasma. Looking at the time-dependent radial velocity we find a correspondence with the peak toroidal mode energies of the MHD instabilities.

Future steps will include modelling the ELM-resolved W source by including sputtering and prompt redeposition effects, and the implementation and verification of neoclassical transport due to impurity-background plasma collisions. This will allow us to perform simulations on longer timescales and simulate impurity accumulation. Also the dependence on ELM amplitude and initial distributions will be investigated.

References
[1] R. Neu et al. In: Fusion Eng. Des. 65.3 SPEC. (2003). DOI : 10.1016/S0920-3796(02)00381-2.
[2] I. Nunes. In: Plasma Phys. Control. Fusion 58.1 (2016). DOI : 10.1088/0741-3335/58/1/014034.
[3] M. R. Wade et al. In: Phys. Rev. Lett. 94.22 (2005). DOI : 10.1103/PhysRevLett.94.225001.
[4] R Dux et al. In: Plasma Phys. Control. Fusion 56.12 (2014). DOI : 10.1088/0741-3335/56/12/124003.
[5] U. Stroth et al, Nucl. Fusion 53, 104003 (2013)
[6] G.T.A. Huysmans and O. Czarrny. In: Nuclear Fusion 47.7 (2007). DOI : 10.1088/0029-5515/47/7/016.
[7] F. Mink, M. Hoelzl et al. Nonlinear coupling induced toroidal structure of edge localized modes. (submitted)
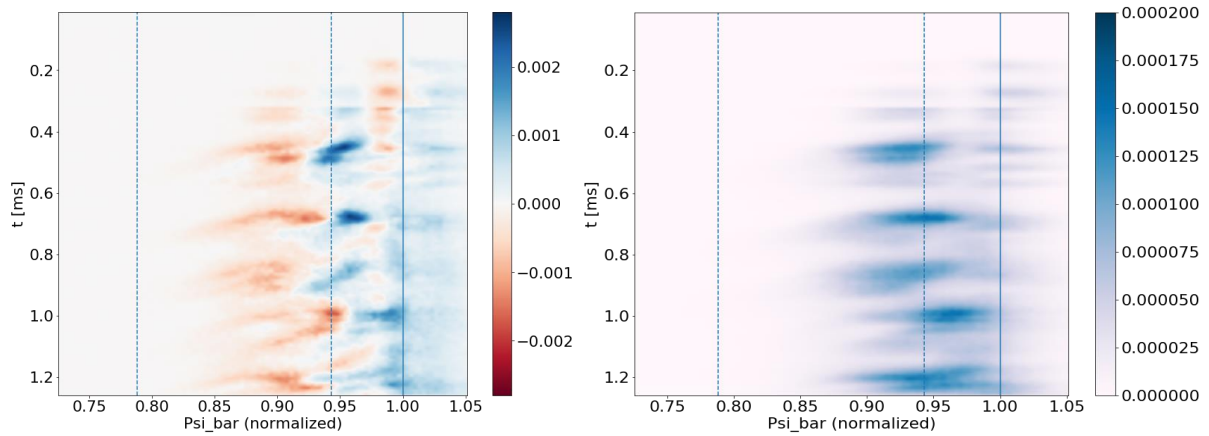
Figure 3 Average and mean-square rate of change of $\overline{\psi}$ for particles at different radial positions and times.
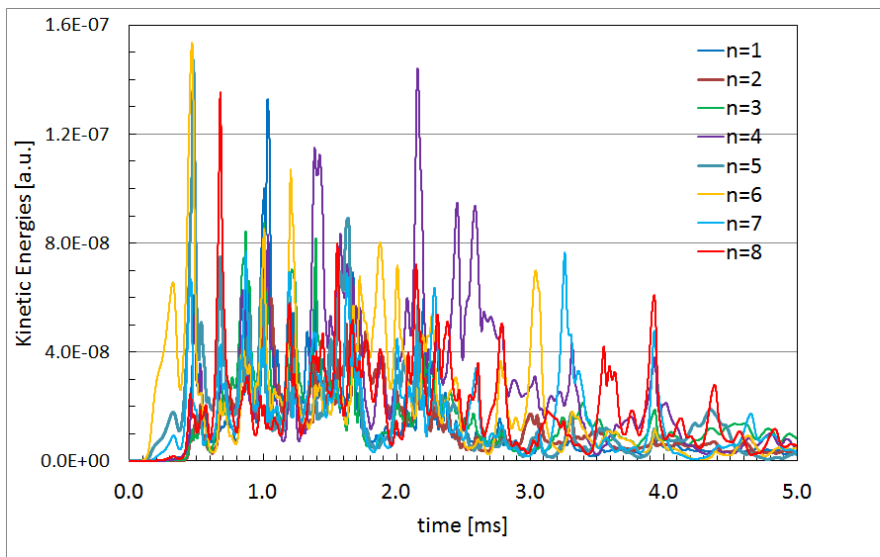
Figure 4: Mode energies as a function of time of the ELM simulation in AUG #33616
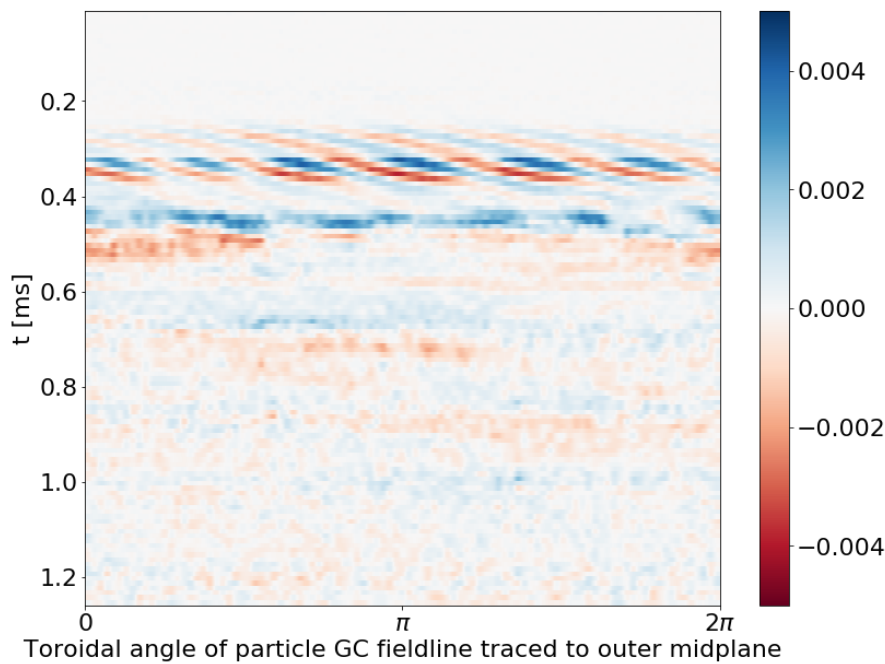
Figure 5 Radial velocity versus fieldline outer midplane toroidal angle φ_0 and time for particles with $\overline{\psi}$ between 0.89 and 0.91.